EVLA Memo #204
The Sensitivity of the EVLA at L (1–2 GHz) and S (2–4 GHz) Bands

Emmanuel Momjian (NRAO)

September 6, 2017

Abstract

Sensitivity measurements of the EVLA at L-band (1–2 GHz) and S-band (2–4 GHz) are presented in this memo. These measurements were carried out after all the EVLA antennas were retrofitted with L-band receivers that utilize the new thermal gap assembly. Furthermore, the S-band measurements constitute the first sensitivity assessment utilizing all the EVLA antennas. Values of sensitivity measurements outside the nominal frequency ranges of these two receiver bands are also reported to demonstrate the feasibility of tuning and the extended performance of each receiver band.

1 Introduction

In 2010, a new thermal gap assembly was implemented on the C-band (4–8 GHz) receiver system of the EVLA. Subsequently, in early 2012 a similar thermal gap assembly was implemented on the L-band (1–2 GHz) receiver system of the EVLA. For L-band, lab measurements showed a clear improvement in the sensitivity below 1.6 GHz and above 1.95 GHz and a small degradation between 1.6 and 1.95 GHz, in both the RCP and LCP, when comparing the performance of a receiver with the new thermal gap assembly versus a receiver with the old thermal gap assembly (see Figure 1 in EVLA Memo #165, Momjian et al. 2012). Furthermore, EVLA Memo #165 presented the impact on the sensitivity of L-band observations using on-the-sky measurements as soon as the new receivers were installed on three EVLA antennas.

By summer 2015 all the antennas in the array were equipped with these L-band receivers. To quantify the sensitivity of the full array with the new thermal gap assembly of the L-band receivers in astronomical observations, on-the-sky test observations were carried out. Similar observations using the S-band (2–4 GHz) receivers were also carried out using all EVLA antennas for the first time and in preparation for the VLA Sky Survey. For reference, Figure 1 shows the lab measurements of the receiver temperature of an EVLA S-band receiver in RCP and LCP as well as the average of the two polarizations.

2 Observations

The EVLA A-configuration observations at L- and S-bands were carried out on August 20, 2015, for a total of 70 minutes. The calibrator source 3C48 (J0137+3309) and a nearby field devoid of strong continuum sources (hereafter "blank field") were observed in this session. For each receiver band, the WIDAR correlator was configured to deliver two different frequency settings to cover the receivers' extended frequency spans with the 8-bit samplers. For L-band, sub-bands with

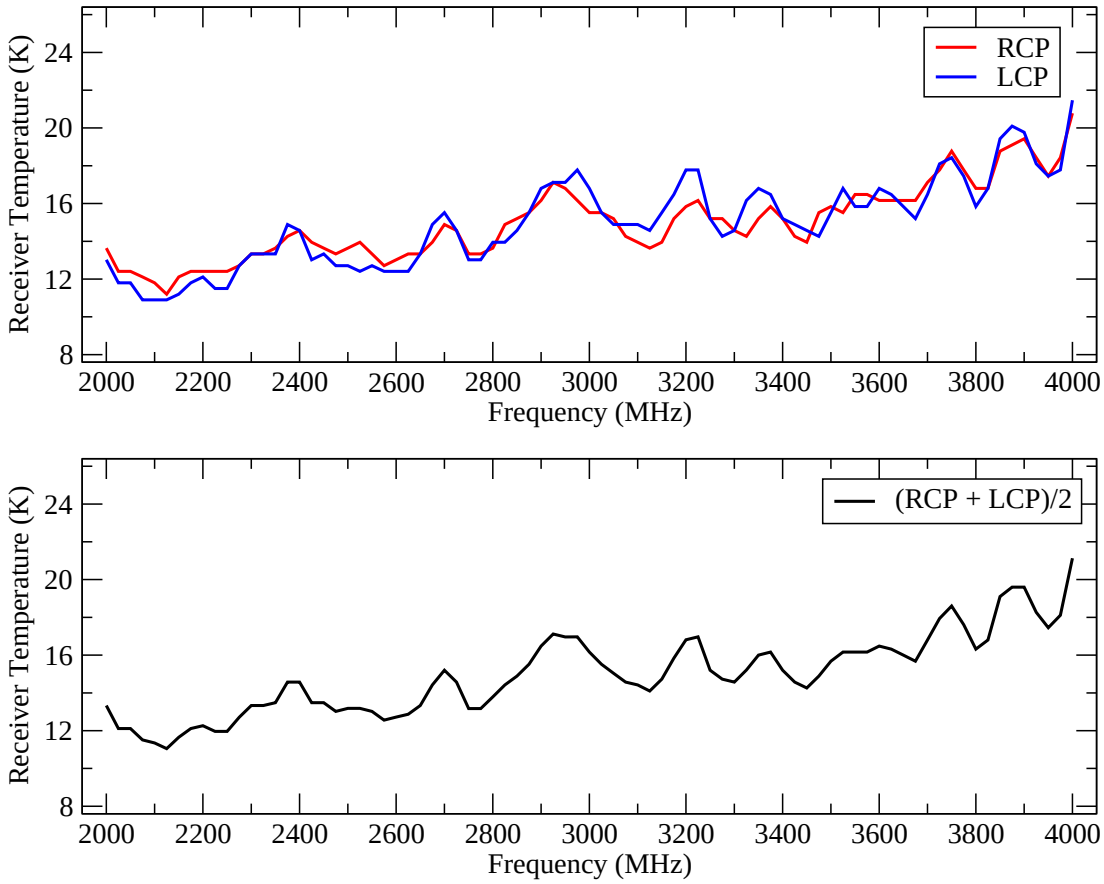

Figure 1: Lab measurements of the receiver temperature of an EVLA S-band receiver in the RCP and LCP separately (*top*), and the average of the two polarizations ([RCP + LCP]/2; *bottom*). The receiver temperature data are courtesy of W. Grammer and the front-end group of the VLA.

bandwidths of 32 MHz with 512 spectral channels were used, resulting in a channel separation of 62.5 kHz, while for S-band the sub-band bandwidths were 128 MHz with 256 spectral channels, resulting in a channel separation of 0.5 MHz. The correlator integration time was set to 5 and 3 seconds, for L- and S-band, respectively.

The frequencies of the two settings per receiver band and of the baseband pairs in each setting were chosen such that the noisier data from the 1st sub-band (i.e., sub-band 0; EVLA Memo #154, Morris & Momjian 2012) could be excluded from this sensitivity assessment without having any gaps in the frequency coverage. The frequency settings of the observations are listed in Table 1, and shown in Figure 2.

The antenna elevations during these observations ranged between ∼56 and 61 degrees at L-band, and between ∼62 and 68 degrees at S-band.

3 Data Reduction and Analysis

Data reduction and analysis were carried out in AIPS. The flux density scale was set using the Perley & Butler 2013 coefficients for 3C48. After applying a priori flagging and excising integrations affected by interference, antenna based delay, complex gain and bandpass calibration solutions were obtained using the data of the calibrator source 3C48 for each sub-band and polarization product (i.e., RR and LL) separately. These solutions were then applied on the visibilities of the blank field,

Setup	Frequency Range (MHz)	
	Baseband Pair A0C0	Baseband Pair B0D0
L1	930–1282	1268–1620
L2	1602–1954	1942–2294
S1	1688–2712	2488–3256
S2	3288–4312	3128–3512

Table 1: Summary of the L-band (1–2 GHz) and S-band (2–4 GHz) frequency settings. Frequencies below and above the nominal ranges of the receivers were included to assess the extended performance of each receiver band.

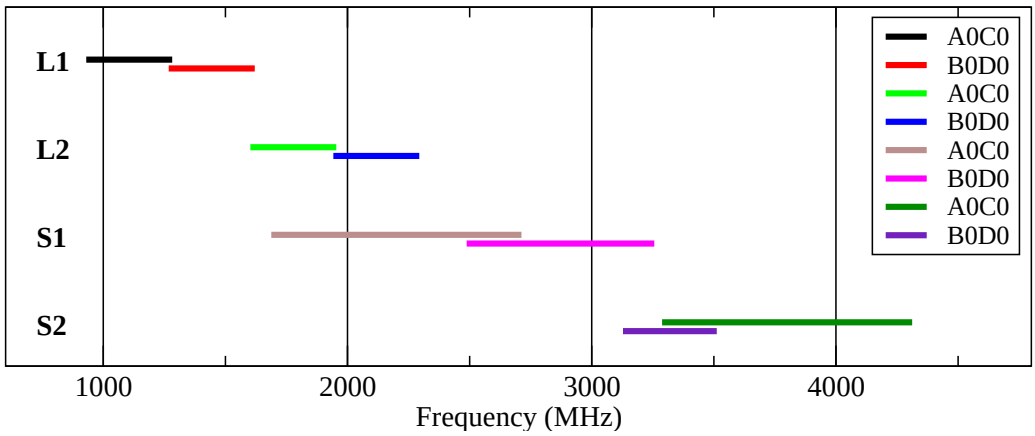

Figure 2: The two instrument configurations used for each of L-band (1–2 GHz) and S-band (2–4 GHz) observations. The indices L1 and L2 for L-band, and S1 and S2 for S-band mark the individual settings and their respective baseband pairs and frequency ranges as listed in Table 1.

and spectra were generated to visually inspect its data in order to further ensure the exclusion of spectral channels that were affected by RFI from subsequent analysis.

Using the AIPS task UVHGM, the RMS noise values for Stokes I were measured by fitting Gaussian profiles on the histogram distributions of the blank field's real part of the visibilities. For this, channels from each sub-band that were not visibly contaminated by RFI were used. A 3-channel Hanning-smoothing was applied on the spectra in all the data reduction and analysis steps to reduce the Gibbs ringing phenomenon introduced by strong RFI features at various L- and S-band frequencies.

The sensitivity measurements reported in this memo are based on the average values of the baselines among all the EVLA antennas. No systematic attempts were made to exclude less sensitive antennas while measuring the RMS noise values in order to provide realistic numbers that are representative of the overall performance of the array, and which can also be utilized in the VLA exposure calculator. However, the noisier sub-band edge channels were excluded to provide non-biased measurements for narrow-band spectral line observations.

As examples of the Gaussian noise in the data, Figure 3 shows histogram distributions of the blank field data using the visibilities of all the baselines from a sub-band at L-band (*left*) and another at S-band (*right*). Also shown are the resulting Gaussian profiles and parameters. The frequency on top of each plot denotes the value at the center of the continuous, RFI-free channel range used to make each plot from a given sub-band.

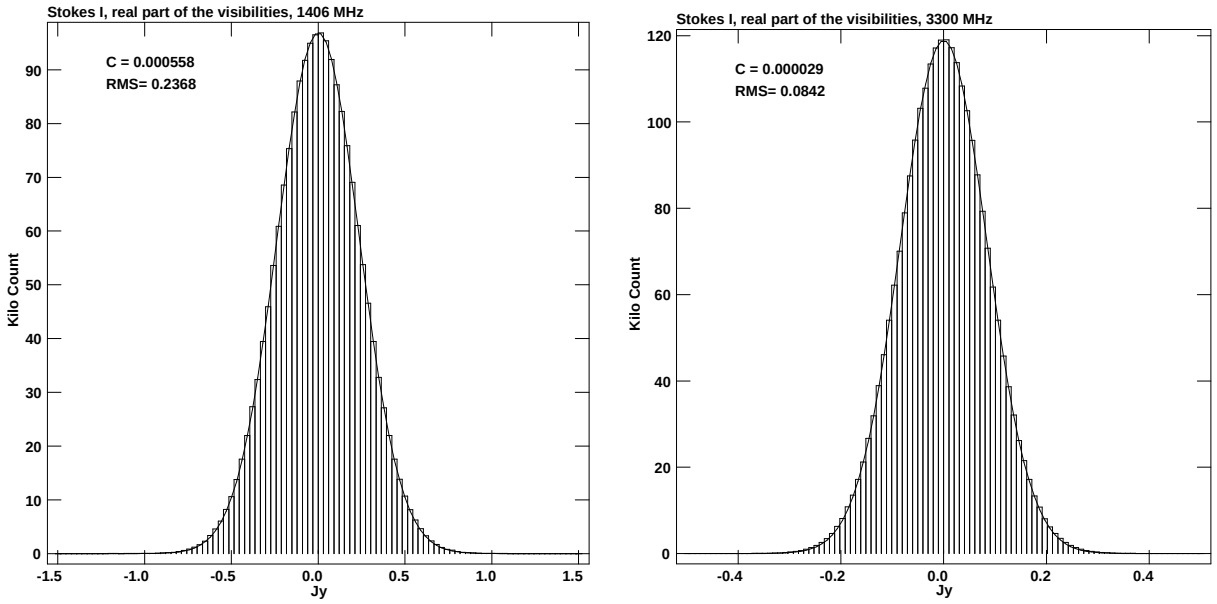

Figure 3: Histogram distributions of the blank field data of all the baselines at L-band (*left*) and S-band (*right*). Also shown are the fitted Gaussian profiles. A continuous, RFI-free channel range from a sub-band at each receiver band, Stokes I, and the real part of the visibilities, were used to make these histograms and measure the RMS noise.

Multiple background continuum sources in the blank field bring frequency dependent contributions to the measured noise values. These sources sum up to as high as $S \sim$138 mJy at the lowest frequencies of L-band, and to as low as $S \sim$0.3 mJy at the highest frequencies of S-band, as determined by imaging all the sub-bands in the data. Frequency dependent corrections were then made to account for these background sources as follows:

$$\mathrm{RMS} = \sqrt{(\mathrm{RMS}_h)^2 - (S)^2}, \tag{1}$$

where RMS_h is the noise value obtained through the histogram fitting for a given frequency range and S is the total flux density in the blank field at that frequency.

The corrected RMS noise values were then converted to System Equivalent Flux Densities (SEFDs) using the following equation:

$$\mathrm{RMS\ (Jy)} = \frac{1}{2\eta_c\kappa_{hs}} \frac{\mathrm{SEFD\ (Jy)}}{\sqrt{\beta\tau}}, \tag{2}$$

where β is the spectral channel width in Hz and τ is the correlator integration time in seconds ($\beta = 62.5 \times 10^3$ Hz and $\tau = 5$ s at L-band, and $\beta = 5 \times 10^5$ Hz and $\tau = 3$ s at S-band). η_c is the WIDAR correlator efficiency, and it is assumed to be 0.936 for the mode used in these observations, and κ_{hs} is the improvement in the signal-to-noise due to the application of the Hanning-smoothing, which is 1.633[1] for a 3-channel Hanning-smoothing.

For the EVLA, note that the SEFD is related to the system temperature (T_{sys}) and the antenna effective area (A_e) by:

[1]The improvement in signal-to-noise due to a 3-channel Hanning-smoothing is $1/\sqrt{0.25^2 + 0.5^2 + 0.25^2}$=1.633

$$\text{SEFD (Jy)} = 5.62\ \frac{T_{\rm sys}\ (\rm K)}{A_e}. \tag{3}$$

4 Results and Discussion

Figures 4 and 5 show the SEFD values in the EVLA L-band (1–2 GHz) and the S-band (2–4 GHz).

For L-band, the SEFD values reported here are mostly higher, on the order of ∼6%, when compared to the SEFD values reported in EVLA Memo #165 (Momjian et al. 2012). However, EVLA Memo #165 was based on measurements obtained using only three antennas; the first three that were equipped with the new thermal gap assembly L-band receivers. Furthermore, in the current work no particular attempt was made to exclude the less sensitive, but perfectly operating antennas at L-band in order to provide numbers that are representative of the overall performance of the array. In fact, L-band Stress Test data centered at 1452 MHz (see EVLA Memo #186; Morris & Momjian 2014, for details regarding the Stress Test) taken on August 19, 2015, which is one day before the observations reported here, show that there is a noticeable distribution in the sensitivities of the antennas, with the least sensitive one being worse by 50% compared to the most sensitive antenna in the array. Therefore, the slightly higher L-band SEFD values reported in this memo may be attributed to the varying sensitivities of the antennas in the array. A similar trend is also seen at S-band, with the least sensitive antenna being worse by 50% compared to the most sensitive antenna.

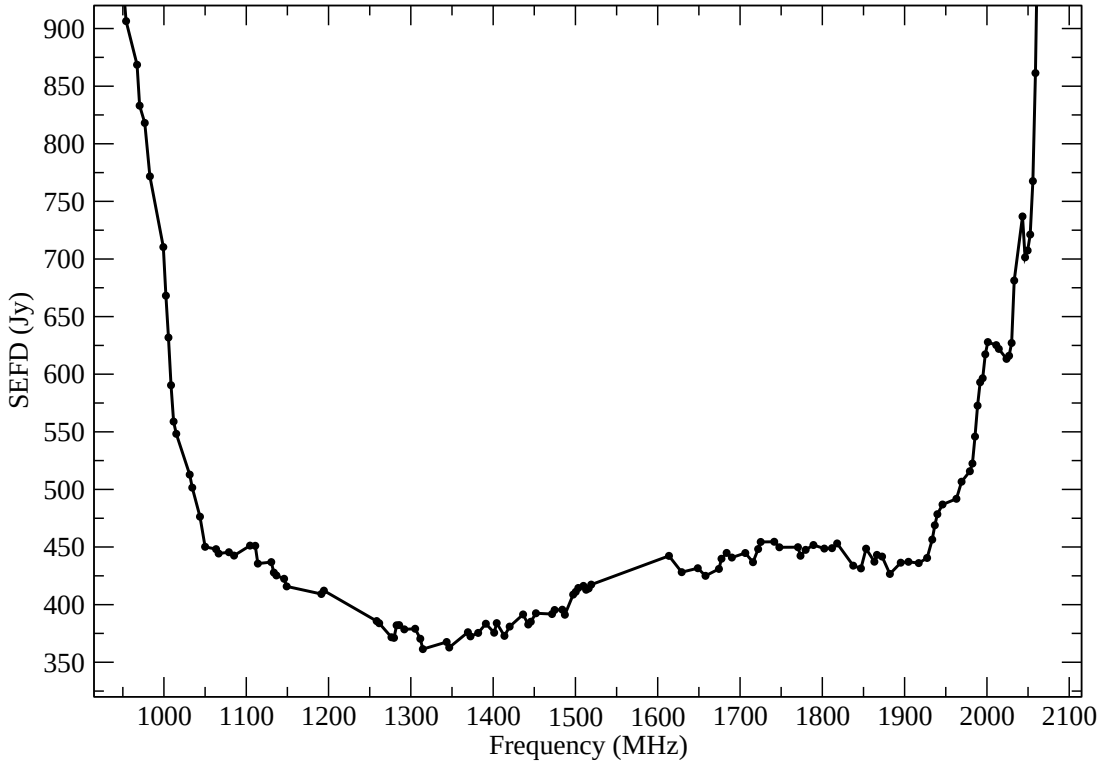

Figure 4: The SEFD values in the nominal EVLA L-band frequency range 1–2 GHz using all the baselines with no particular attempt to exclude the less sensitive, but perfectly operating antennas.

To illustrate the variation in the sensitivity of the antennas at L-band, Figure 6−*top* shows the normalized sensitivity distribution at 1452 MHz using the August 19, 2015, Stress Test results.

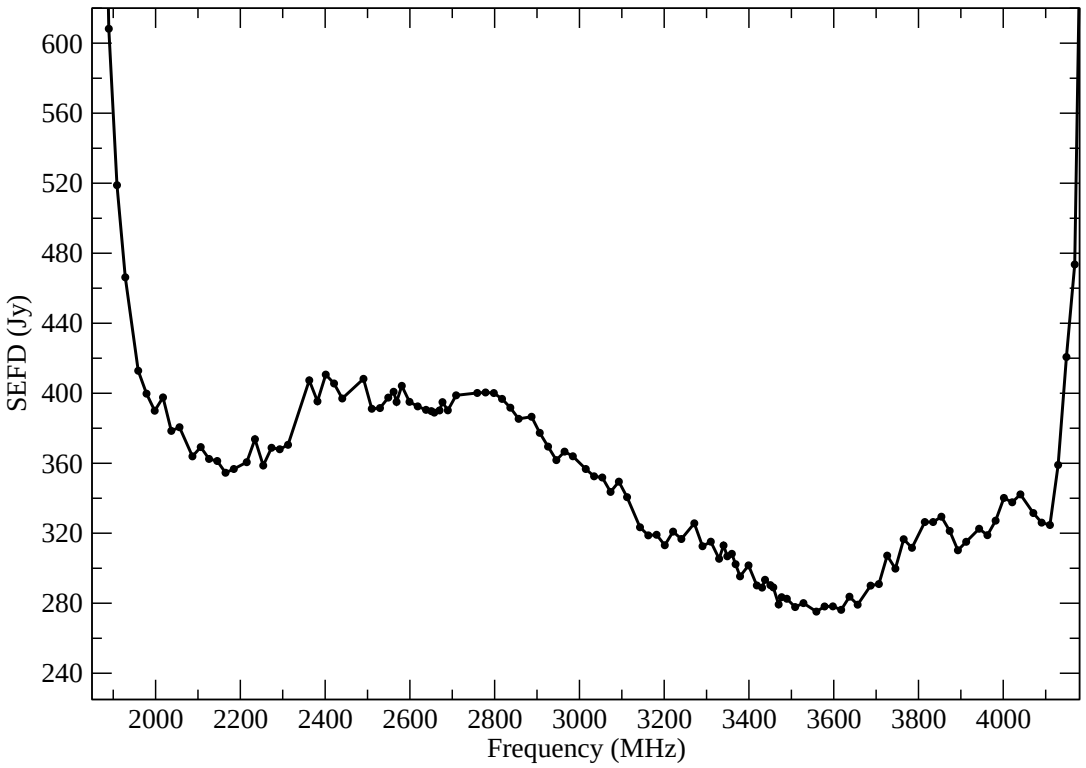

Figure 5: The SEFD values in the nominal EVLA S-band frequency range 2–4 GHz using all the baselines with no particular attempt to exclude the less sensitive, but perfectly operating antennas.

Figure 6−*bottom* provides a similar distribution of the EVLA antennas at S-band at 3084 MHz. The sensitivity values are normalized by the overall mean per band, with the lower numbers reflecting the more sensitive antennas, and the higher numbers the less sensitive ones.

For S-band, and contrary to the lab measurements presented in Figure 1, where the receiver temperature shows almost a linearly increasing trend from 2 to 4 GHz, the on-the-sky SEFD measurements (Figure 5) show a degradation in the sensitivity (higher SEFD values) in the lower half of the band, and in particular in the frequency range 2300 and 2900 MHz. This loss in sensitivity is most likely caused by a drop in the antenna efficiency, whose origin presumably lies in the feed horn illumination pattern. A similar trend is also seen at C-band and is attributed to the same origin as reported in EVLA Memo #188 (Momjian 2014).

As noted in Table 1 and Figure 2, the on-the-sky observations included frequency tunings that are outside the nominal ranges of both the L-band (1–2 GHz) and the S-band (2–4 GHz) receivers. Even though it is possible to tune the L-band receivers down to 935 MHz and up to 2150 MHz, a significant loss in sensitivity is seen below 950 MHz and above 2070 MHz as shown in Figure 7. Similarly, at S-band it is possible to tune down to 1830 MHz and up to 4260 MHz, with a significant loss in sensitivity below 1875 MHz and above 4200 MHz as shown in Figure 8. Therefore, observations below and above these noted frequencies using the L- and S-band receivers should be avoided.

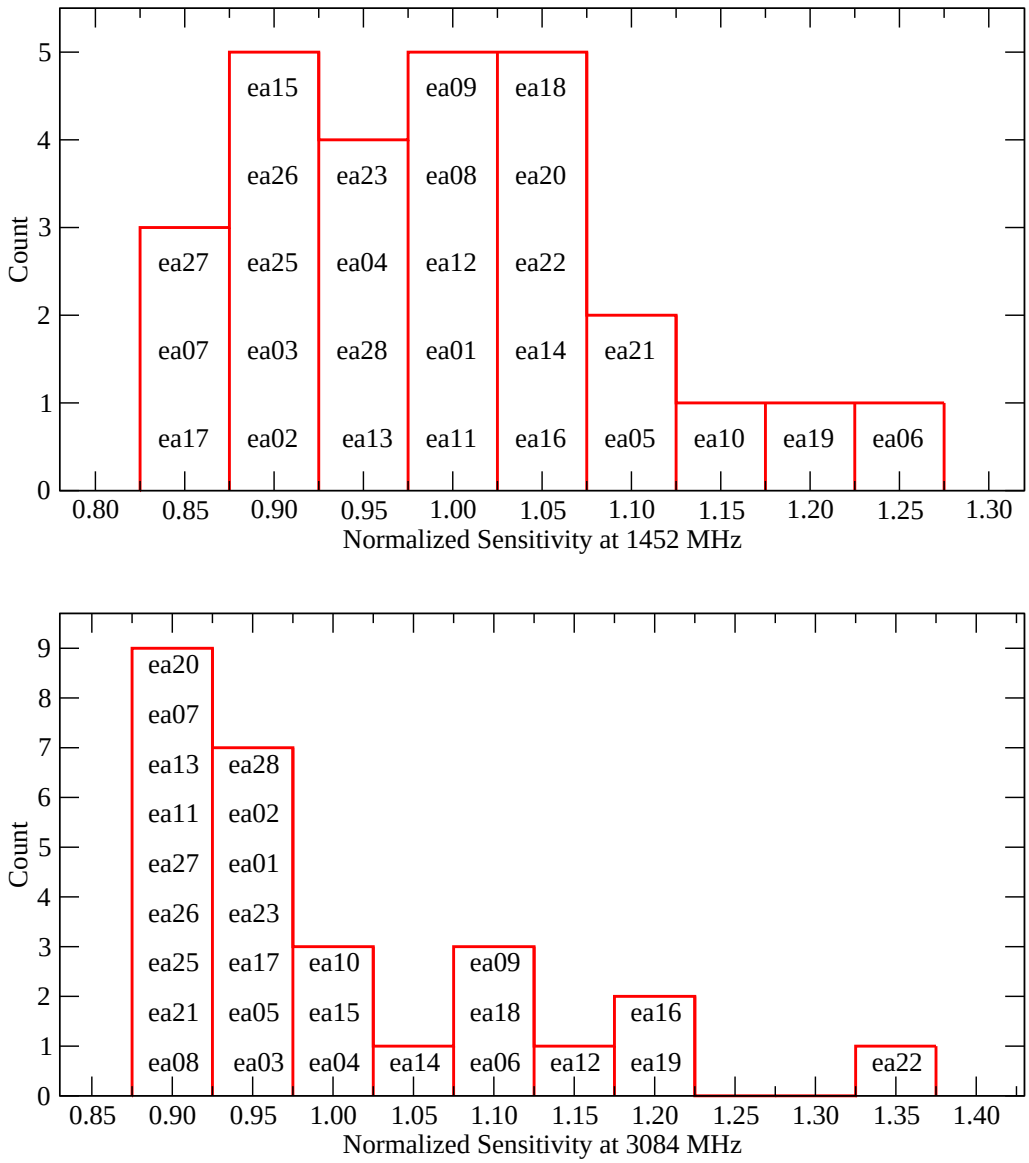

Figure 6: The sensitivity distribution of the EVLA antennas at 1452 MHz (L-band; *top*), and 3084 MHz (S-band; *bottom*) using the Stress Test results of August 19, 2015. The sensitivity values are normalized by the overall mean of all the antennas per band. The lower normalized sensitivity numbers reflect the more sensitive antennas.

5 Acknowledgements

The author would like to thank W. Grammer for providing the lab measurements of the S-band receiver temperature, and R. Perley for very helpful comments and discussions.

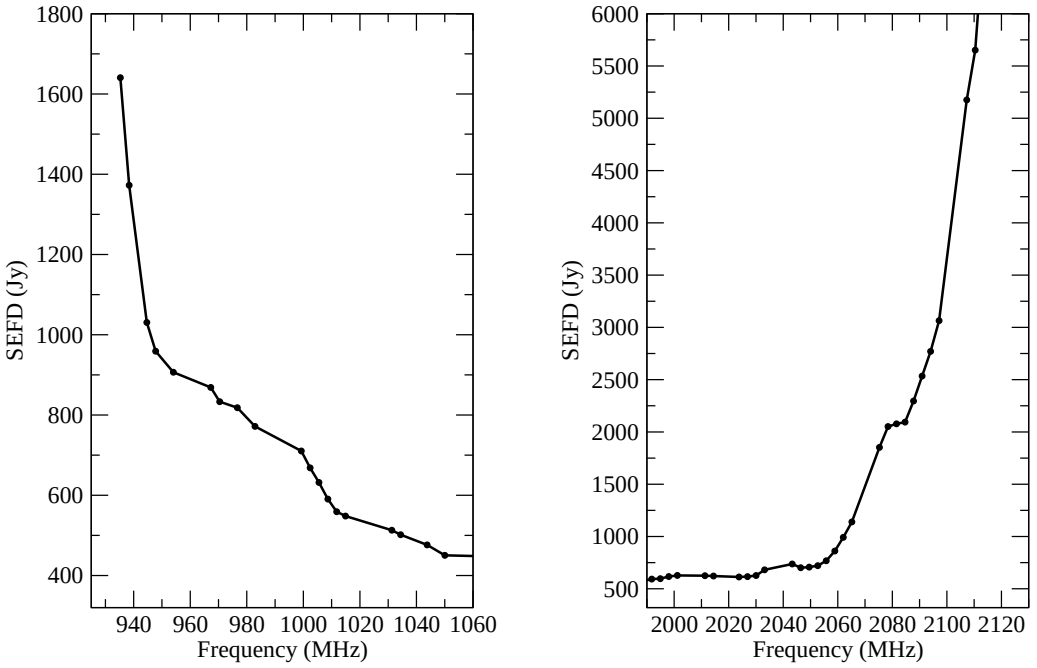

Figure 7: The SEFD values below (*left*) and above (*right*) the nominal frequency range of the EVLA L-band (1–2 GHz) receiver. A significant loss in sensitivity can be seen below 950 MHz and above 2070 MHz. Observations below and above these frequencies using the L-band receivers should be avoided.

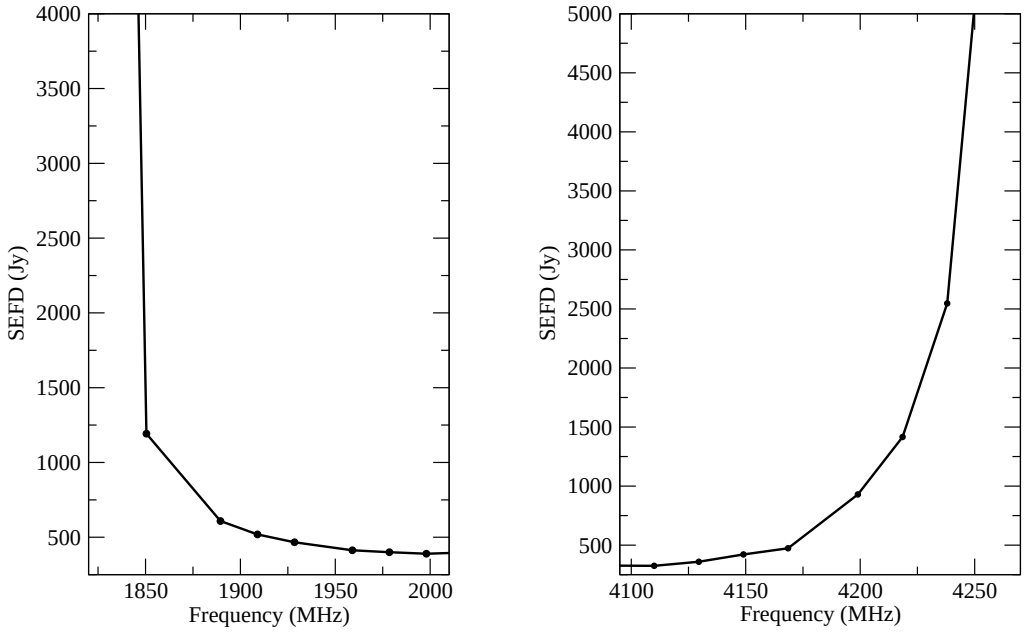

Figure 8: The SEFD values below (*left*) and above (*right*) the nominal frequency range of the EVLA S-band (2–4 GHz) receiver. A significant loss in sensitivity can be seen below 1875 MHz and above 4200 MHz. Observations below and above these frequencies using the S-band receivers should be avoided.